

FIGURE 5.1. The top left panel shows a piecewise constant function fit to some artificial data. The broken vertical lines indicate the positions of the two knots ξ_1 and ξ_2 . The blue curve represents the true function, from which the data were generated with Gaussian noise. The remaining two panels show piecewise linear functions fit to the same data—the top right unrestricted, and the lower left restricted to be continuous at the knots. The lower right panel shows a piecewise-

Piecewise Cubic Polynomials

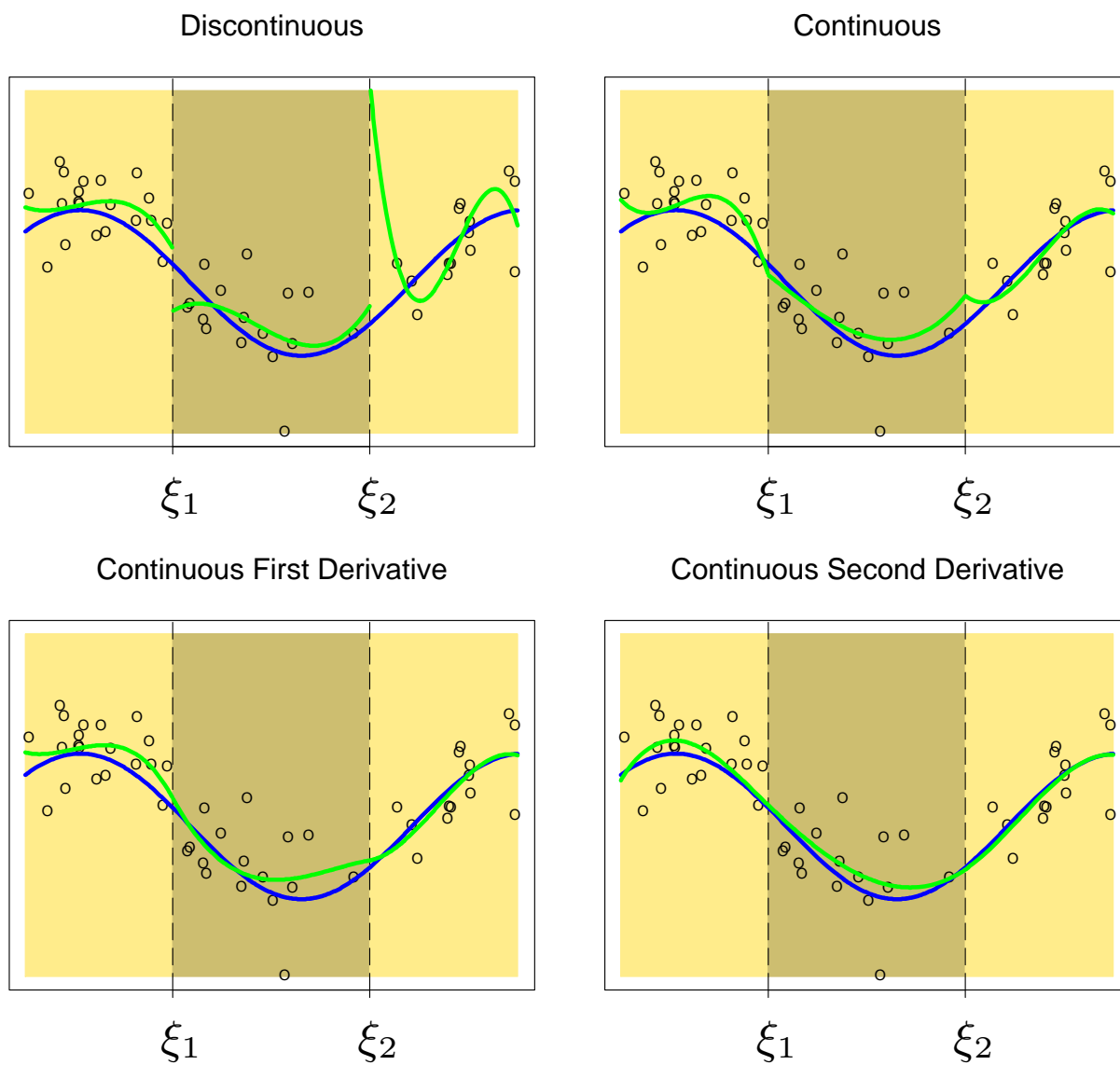


FIGURE 5.2. A series of piecewise-cubic polynomials, with increasing orders of continuity.

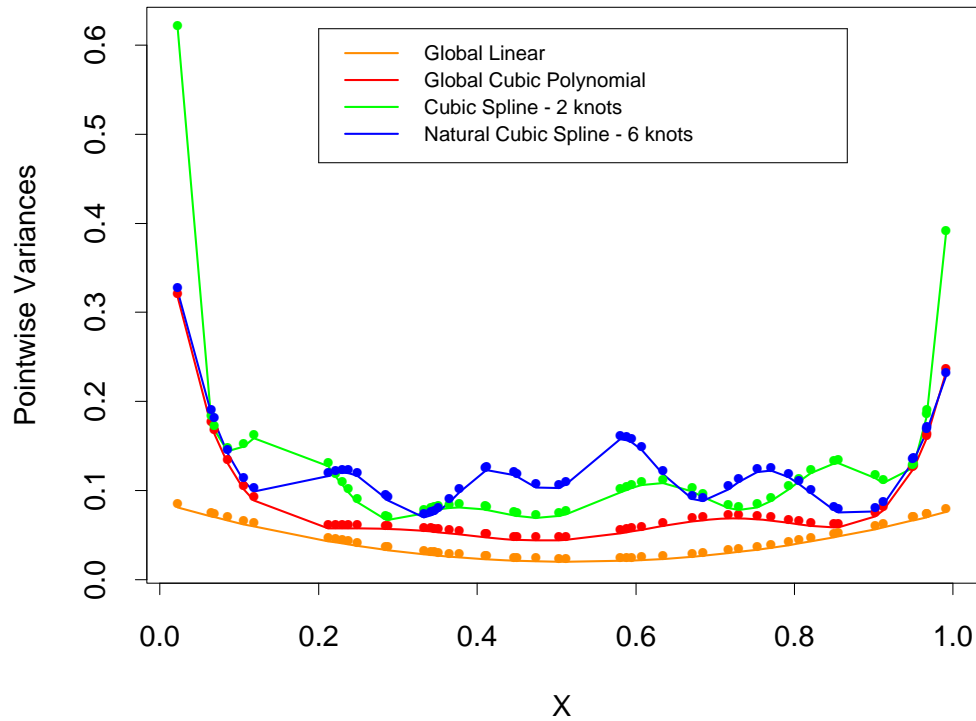


FIGURE 5.3. *Pointwise variance curves for four different models, with X consisting of 50 points drawn at random from $U[0, 1]$, and an assumed error model with constant variance. The linear and cubic polynomial fits have two and four degrees of freedom, respectively, while the cubic spline and natural cubic spline each have six degrees of freedom. The cubic spline has two knots at 0.33 and 0.66, while the natural spline has boundary knots at 0.1 and 0.9, and four interior knots uniformly spaced between them.*

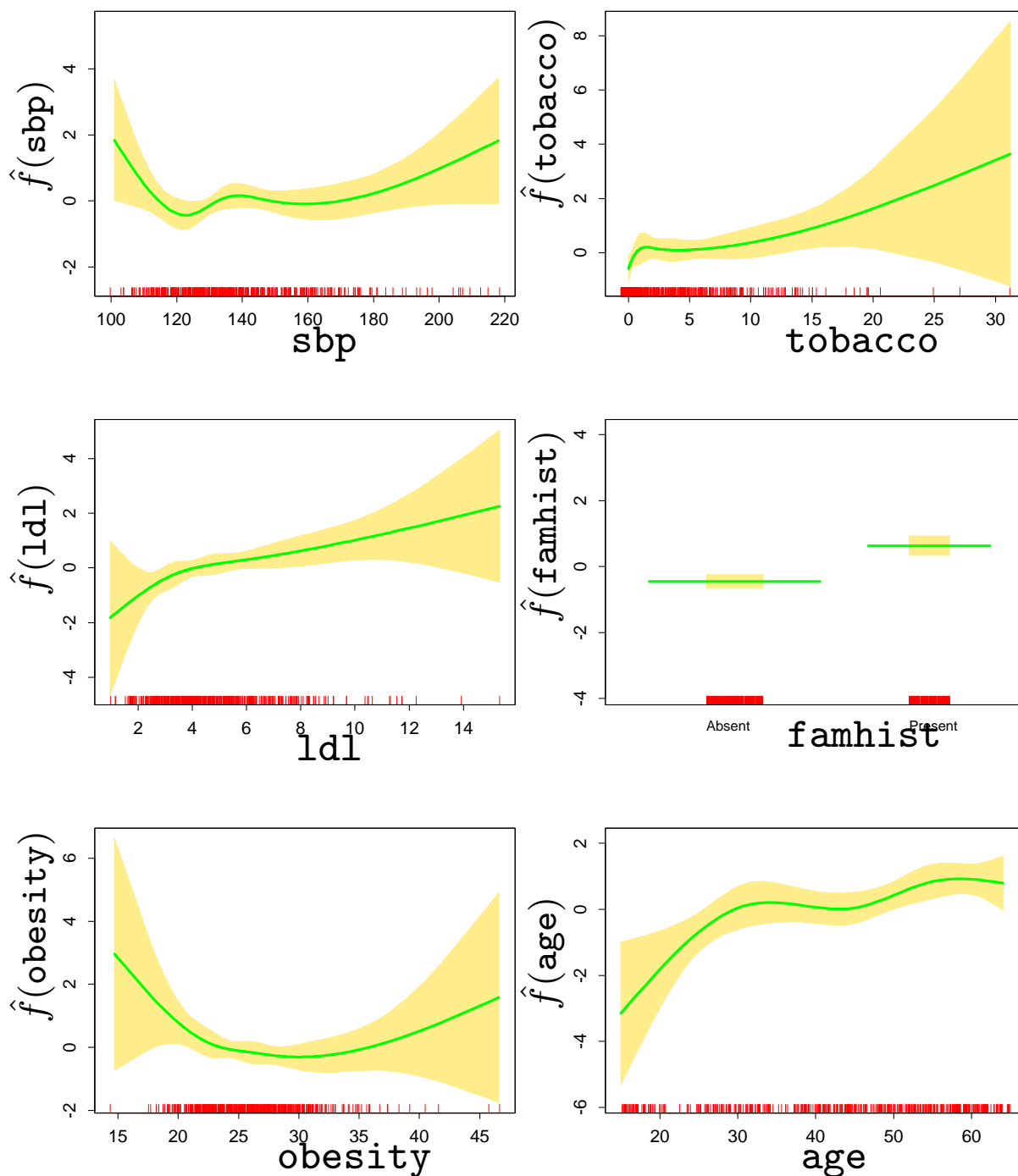


FIGURE 5.4. *Fitted natural-spline functions for each of the terms in the final model selected by the stepwise procedure. Included are pointwise standard-error bands. The rug plot at the base of each figure indicates the location of each of the sample values for that variable (jittered to break ties)*

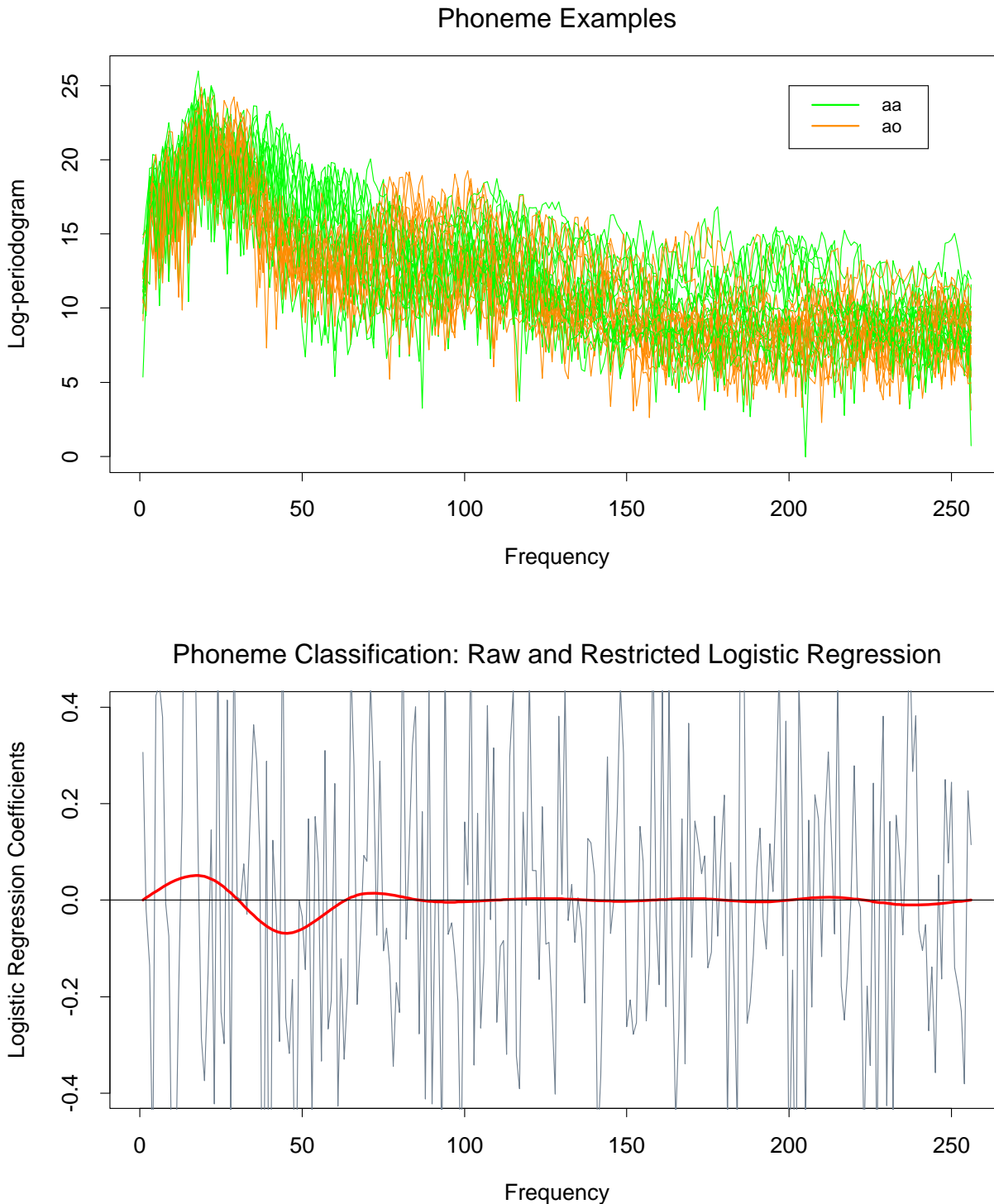


FIGURE 5.5. The top panel displays the log-periodogram as a function of frequency for 15 examples each of the phonemes “aa” and “ao” sampled from a total of 695 “aa”s and 1022 “ao”s. Each log-periodogram is measured at 256 uniformly spaced frequencies. The lower panel shows the coefficients (as a function of fre

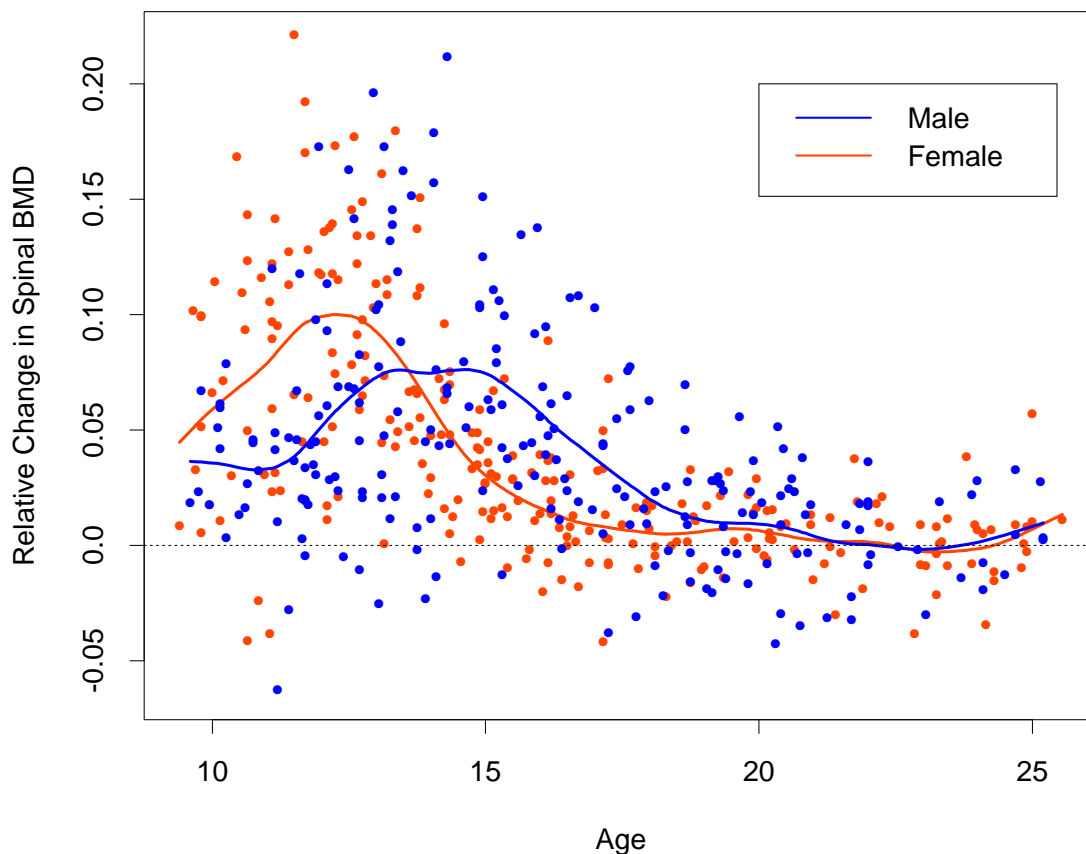


FIGURE 5.6. *The response is the relative change in bone mineral density measured at the spine in adolescents, as a function of age. A separate smoothing spline was fit to the males and females, with $\lambda \approx 0.00022$. This choice corresponds to about 12 degrees of freedom.*

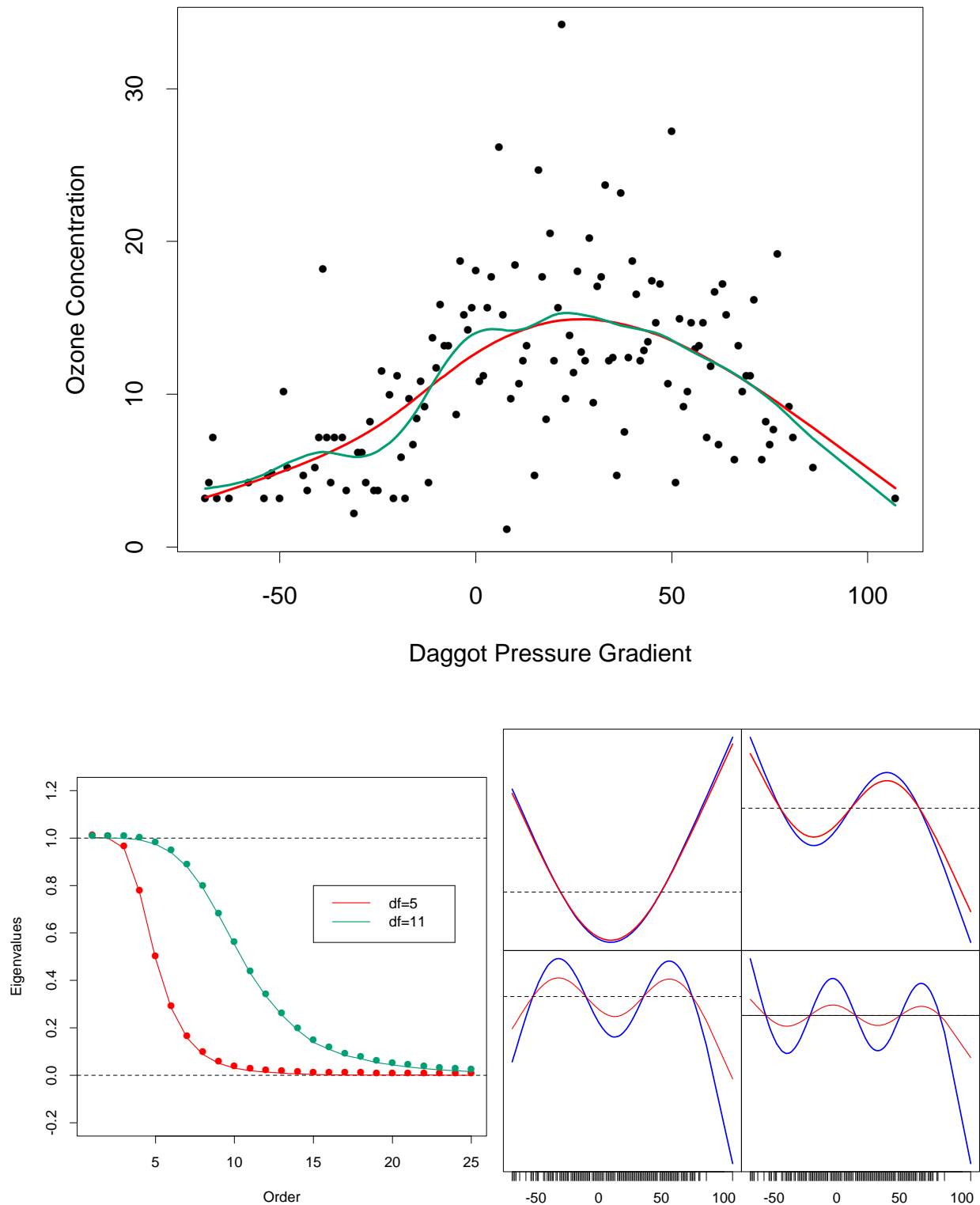


FIGURE 5.7. (Top:) Smoothing spline fit of ozone concentration versus Daggot pressure gradient. The two fits correspond to different values of the smoothing parameter, chosen to achieve five and eleven effective degrees of freedom, defined by $df_\lambda = \text{trace}(\mathbf{S}_\lambda)$. (Lower

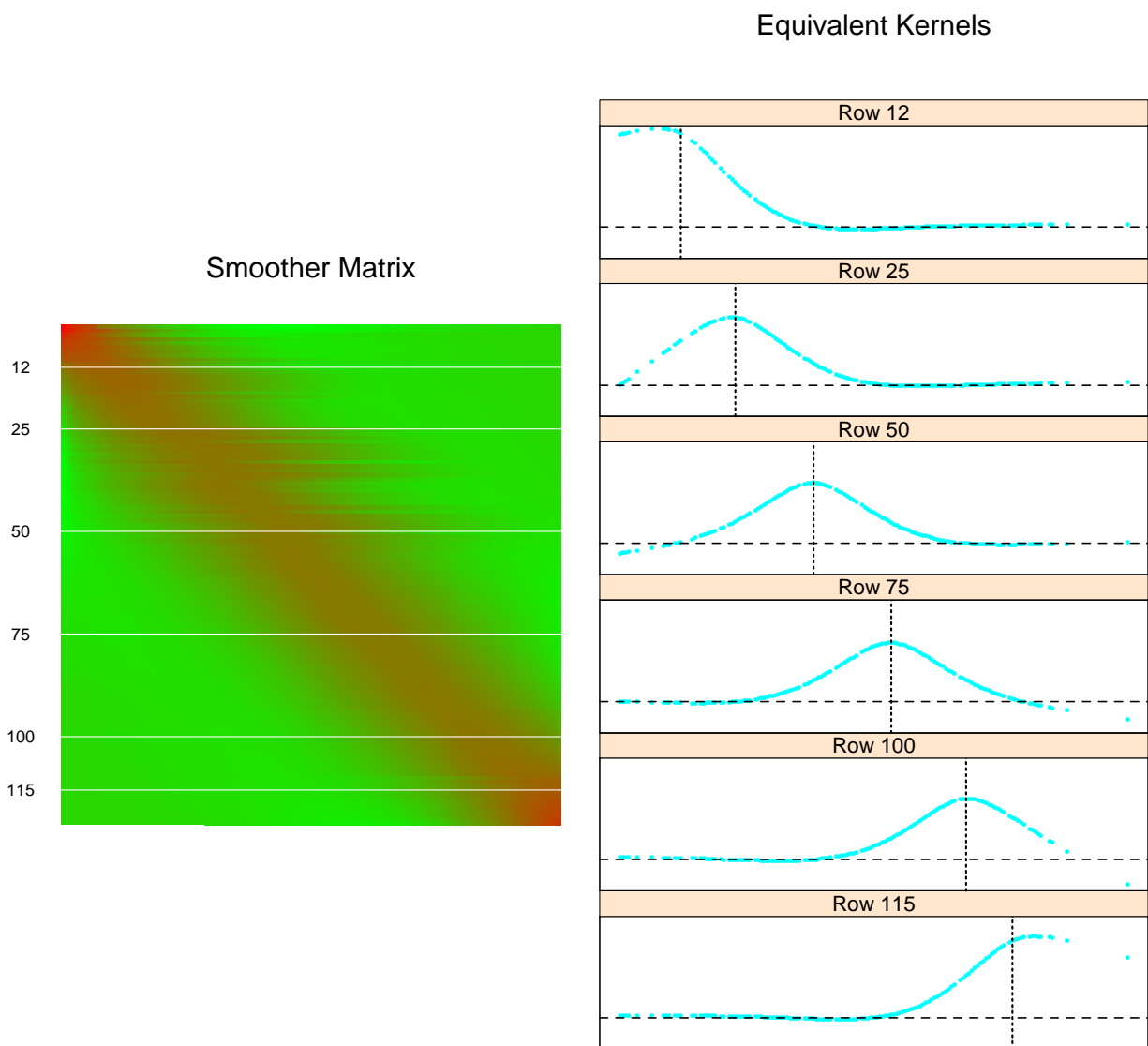


FIGURE 5.8. *The smoother matrix for a smoothing spline is nearly banded, indicating an equivalent kernel with local support. The left panel represents the elements of S as an image. The right panel shows the equivalent kernel or weighting function in detail for the indicated rows.*

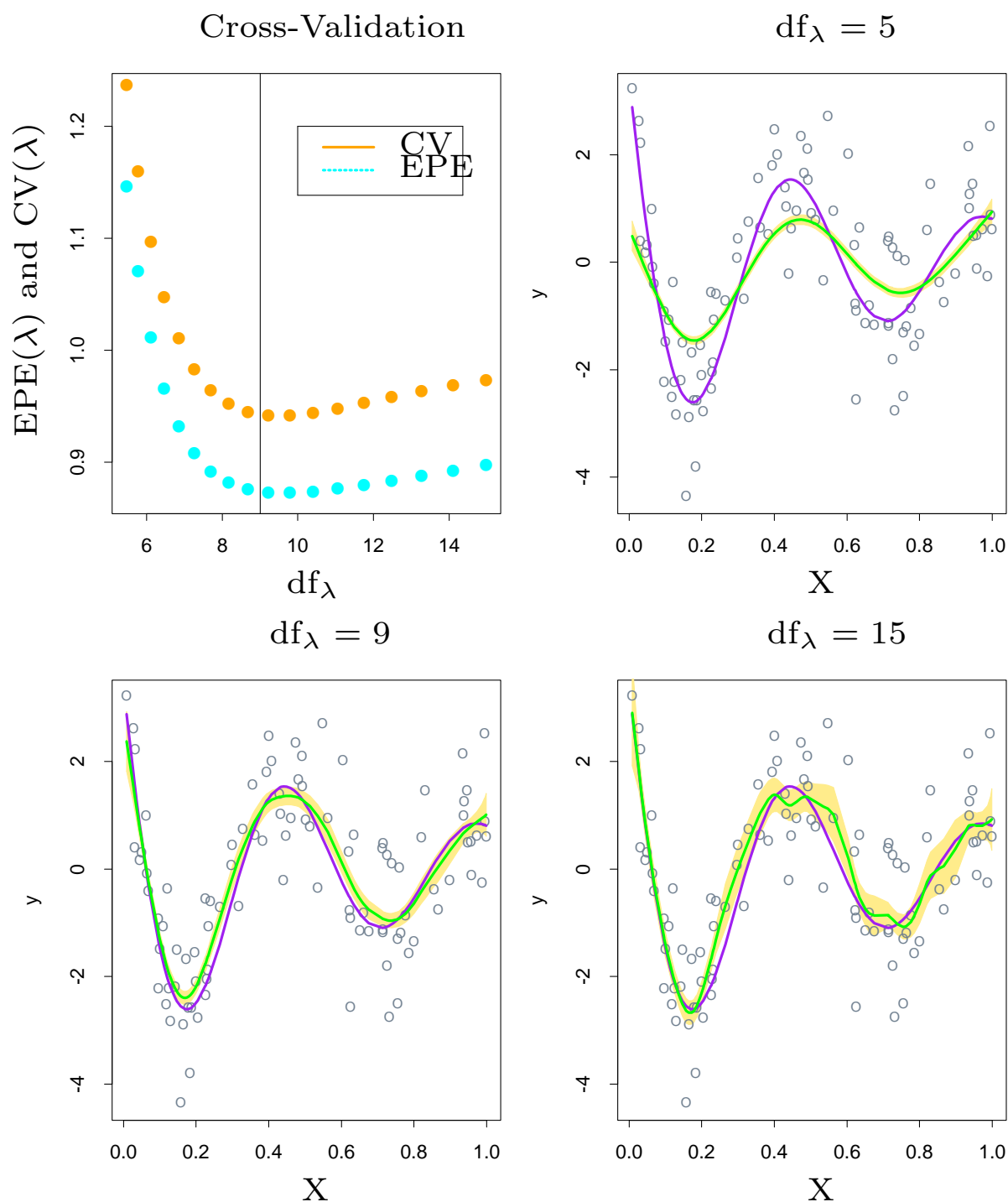


FIGURE 5.9. The top left panel shows the $EPE(\lambda)$ and $CV(\lambda)$ curves for a realization from a nonlinear additive error model (5.22). The remaining panels show the data, the true functions (in purple), and the fitted curves (in green) with yellow shaded $\pm 2 \times$ standard error bands, for three different values of df_λ .

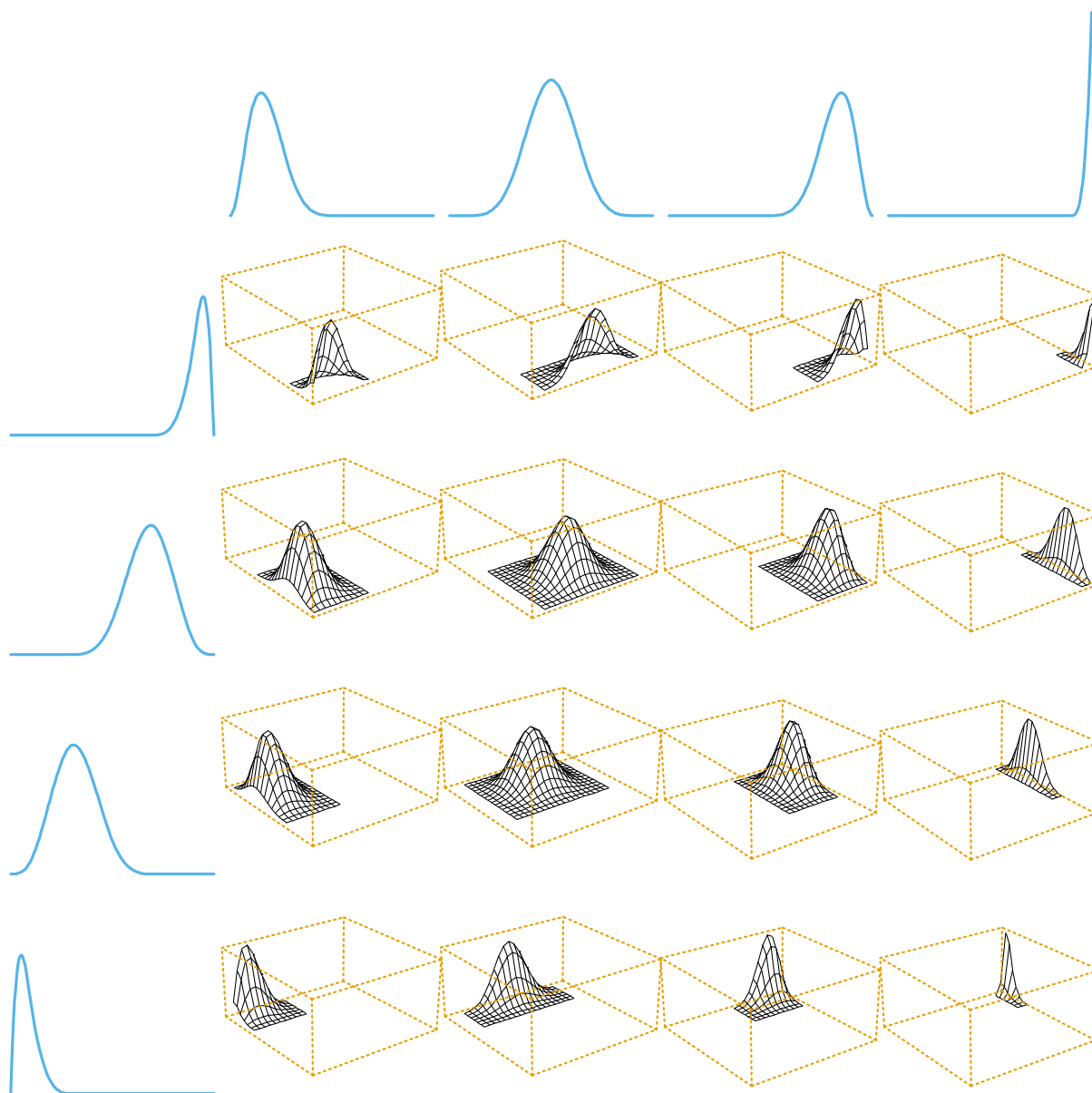
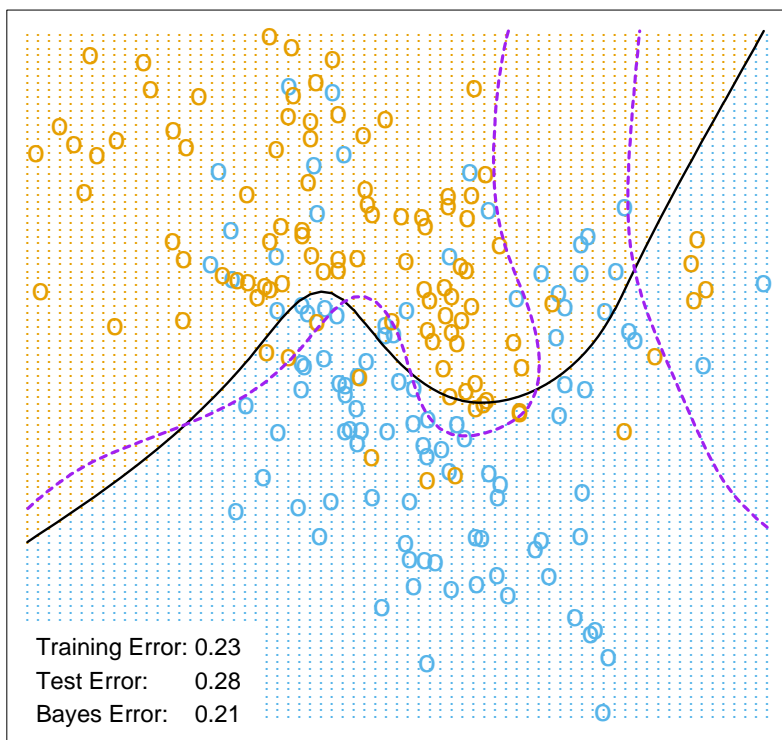


FIGURE 5.10. *A tensor product basis of B-splines, showing some selected pairs. Each two-dimensional function is the tensor product of the corresponding one dimensional marginals.*

Additive Natural Cubic Splines - 4 df each



Natural Cubic Splines - Tensor Product - 4 df each

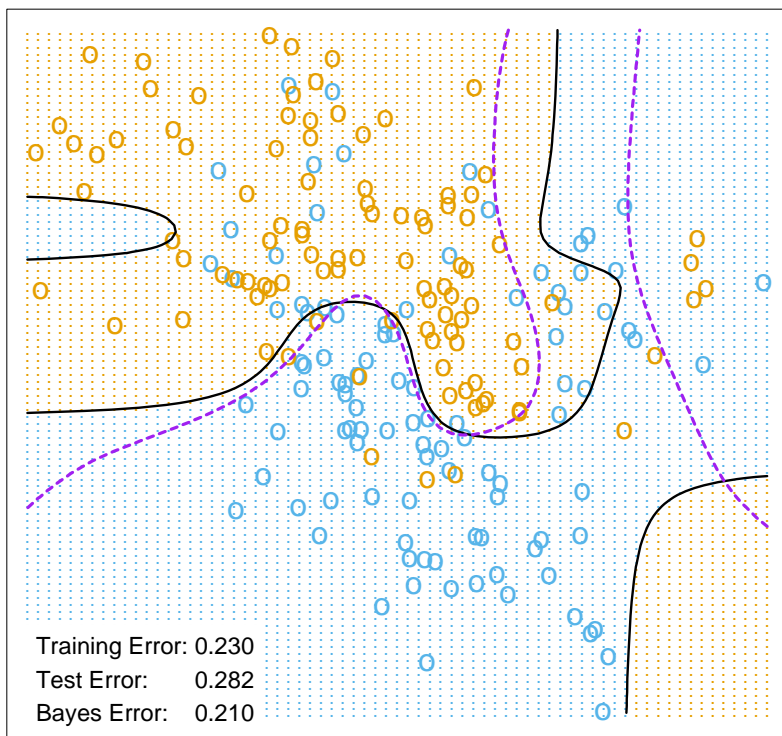


FIGURE 5.11. *The simulation example of Figure 2.1. The upper panel shows the decision bound-*

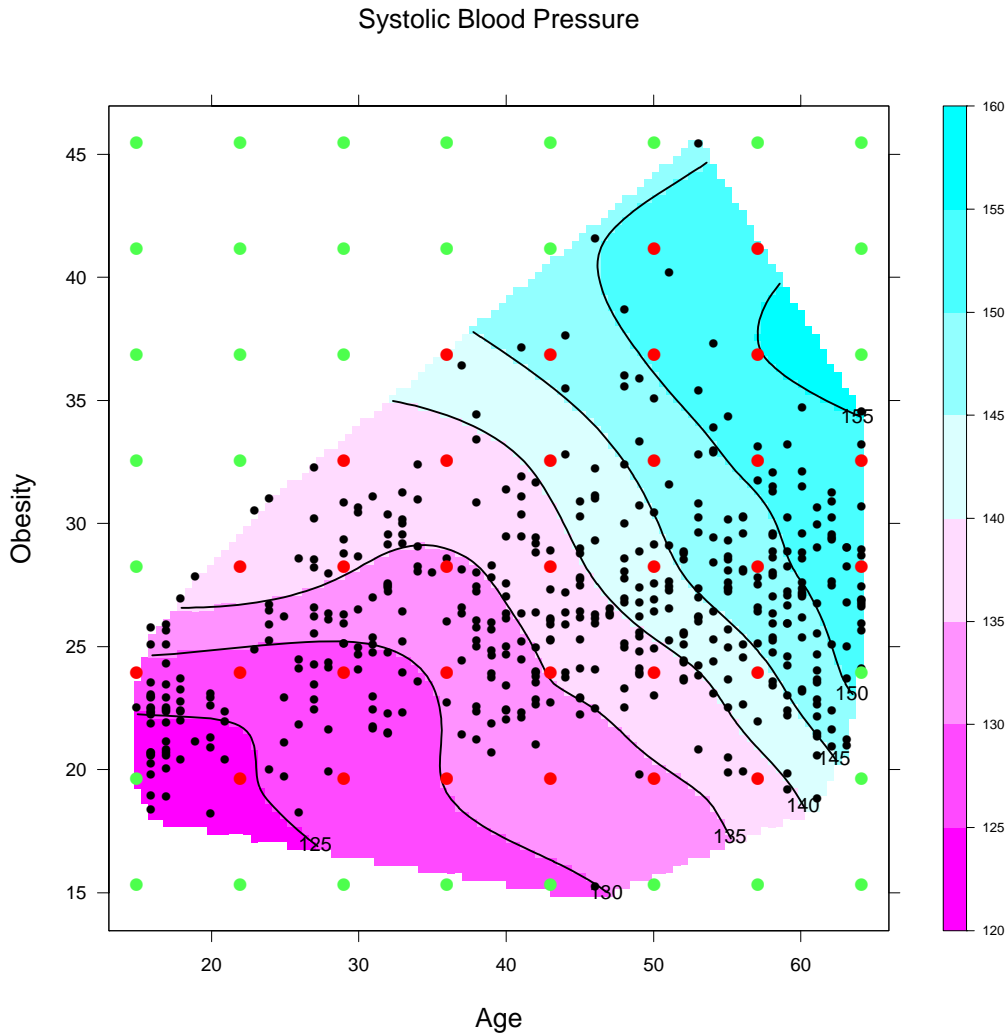


FIGURE 5.12. A thin-plate spline fit to the heart disease data, displayed as a contour plot. The response is systolic blood pressure, modeled as a function of age and obesity. The data points are indicated, as well as the lattice of points used as knots. Care should be taken to use knots from the lattice inside the convex hull of the data (red), and ignore those outside (green).

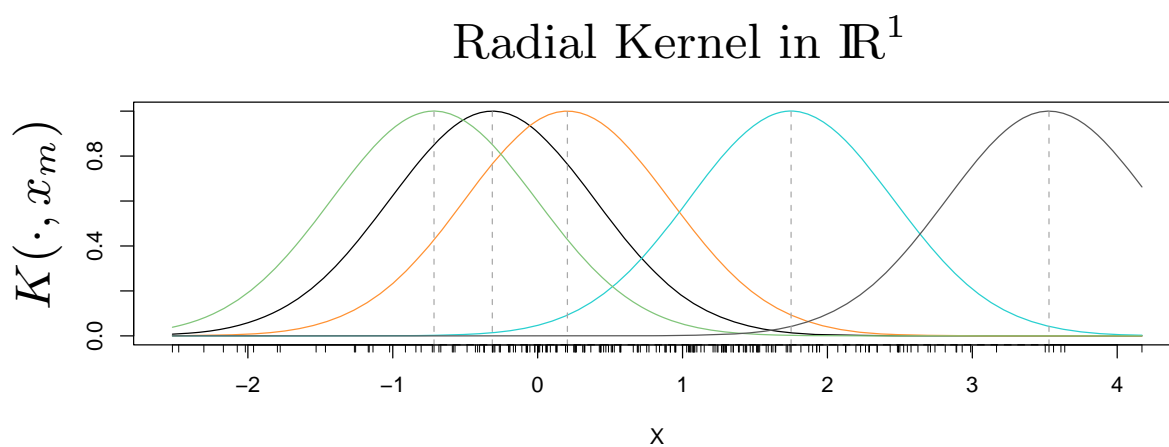


FIGURE 5.13. Radial kernels $k_k(x)$ for the mixture data, with scale parameter $\nu = 1$. The kernels are centered at five points x_m chosen at random from the 200.

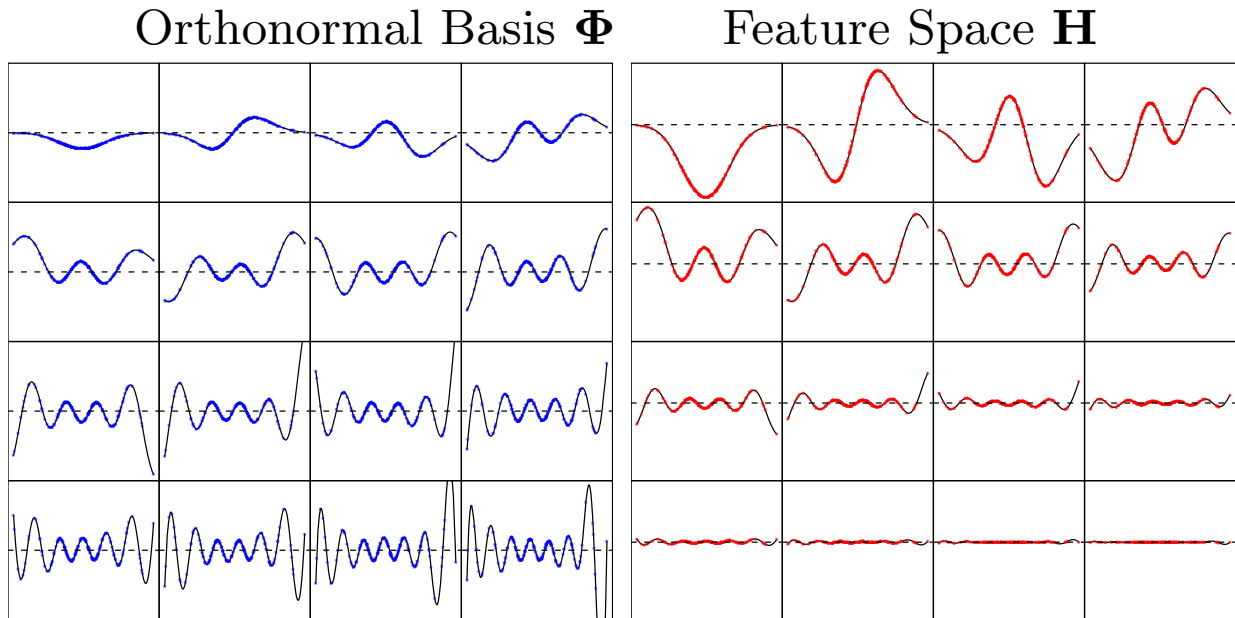


FIGURE 5.14. (Left panel) The first 16 normalized eigenvectors of \mathbf{K} , the 200×200 kernel matrix for the first coordinate of the mixture data. These are viewed as estimates $\hat{\phi}_\ell$ of the eigenfunctions in (5.45), and are represented as functions in \mathbb{R}^1 with the observed values superimposed in color. They are arranged in rows, starting at the top left. (Right panel) Rescaled versions $h_\ell = \sqrt{\hat{\gamma}_\ell} \hat{\phi}_\ell$ of the functions in the left panel, for which the kernel computes the “inner product.”

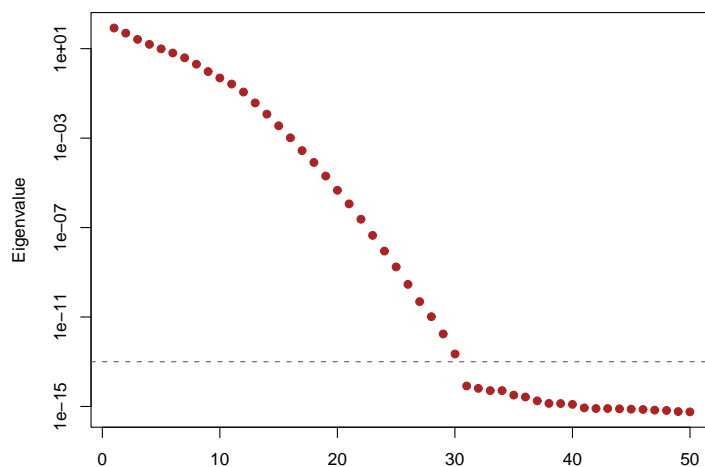


FIGURE 5.15. *The largest 50 eigenvalues of \mathbf{K} ; all those beyond the 30th are effectively zero.*

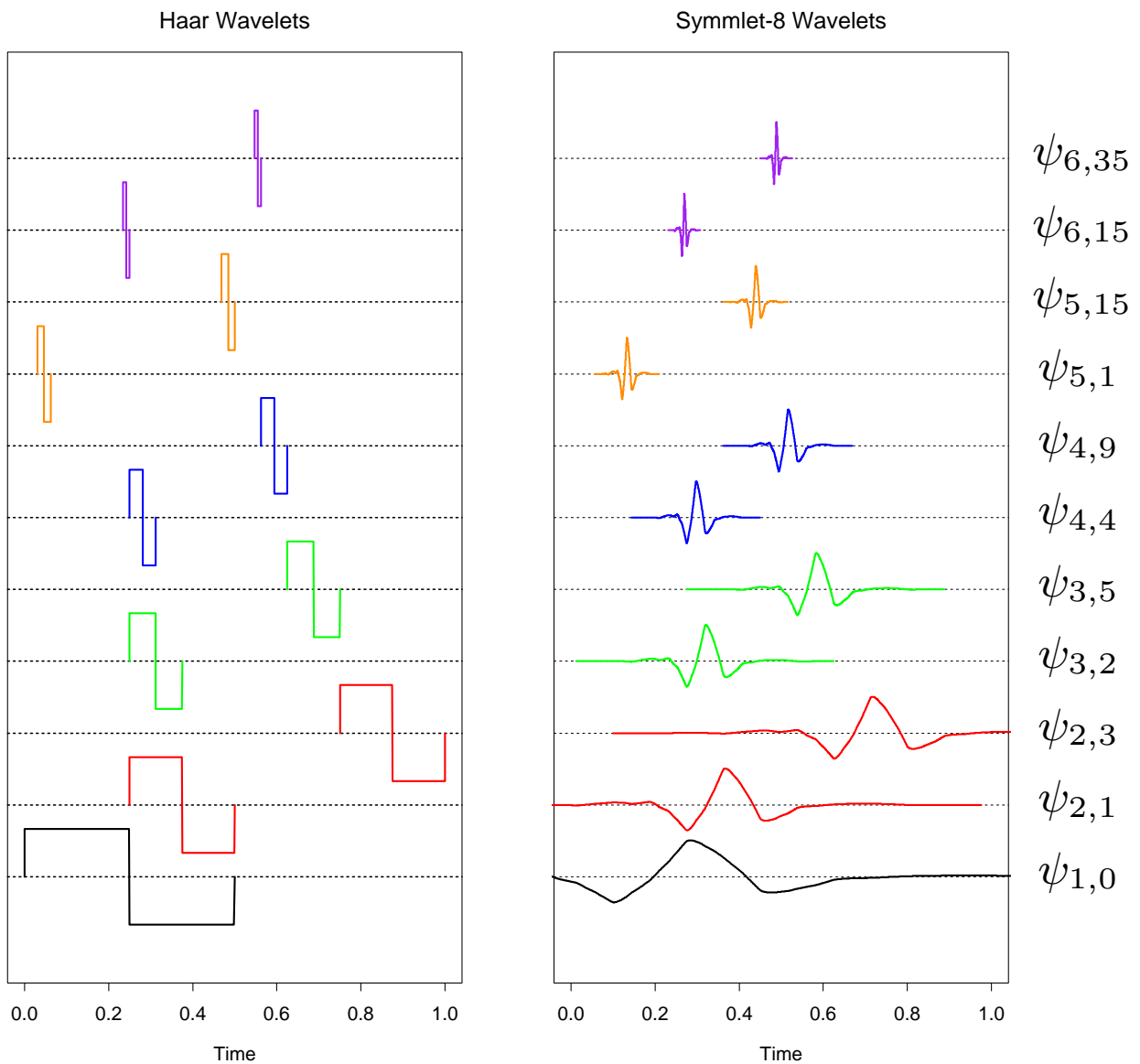


FIGURE 5.16. *Some selected wavelets at different translations and dilations for the Haar and symmlet families. The functions have been scaled to suit the display.*

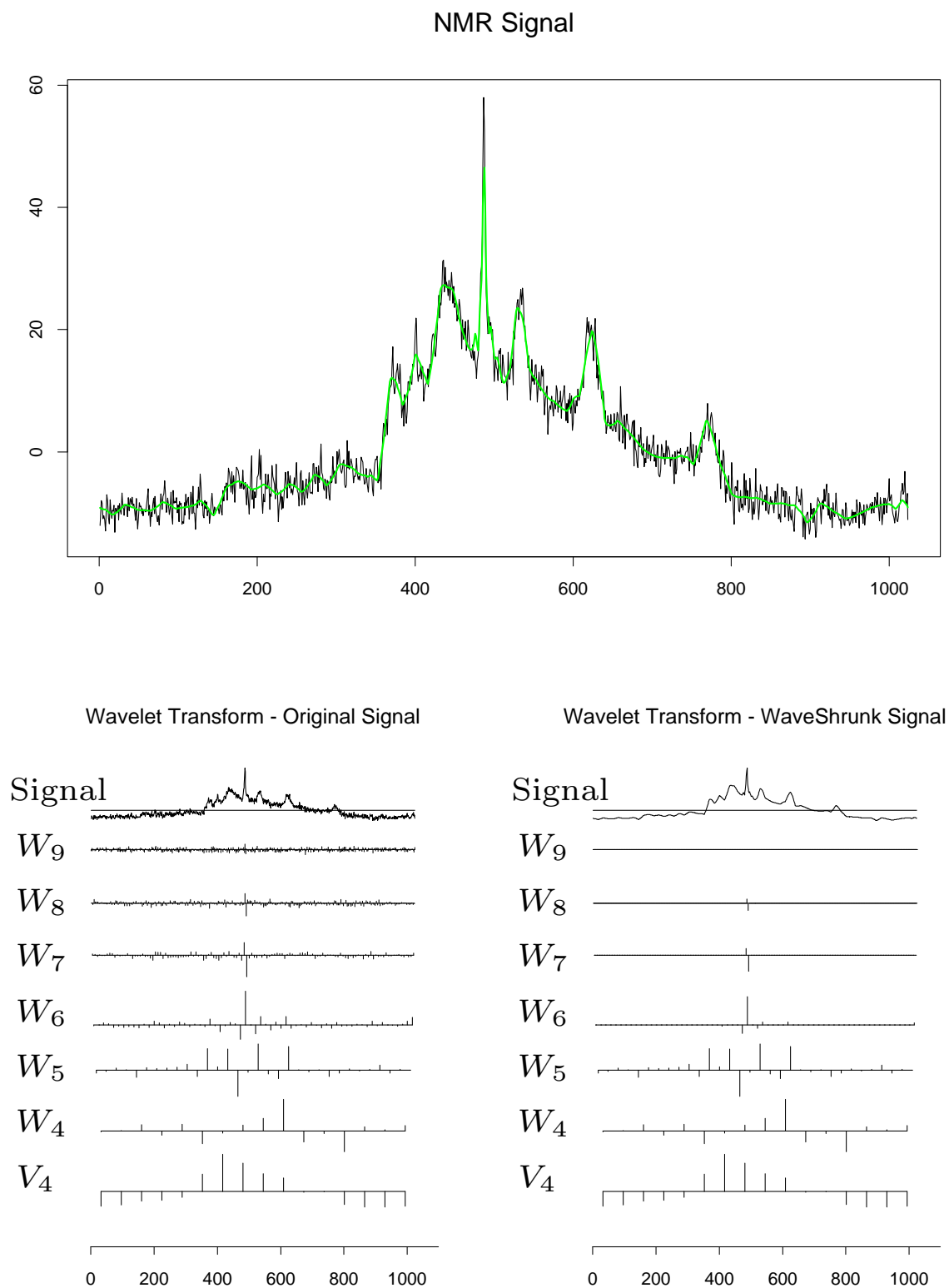


FIGURE 5.17. The top panel shows an NMR signal, with the wavelet-shrunk version superimposed in green. The lower left panel represents the wavelet trans-

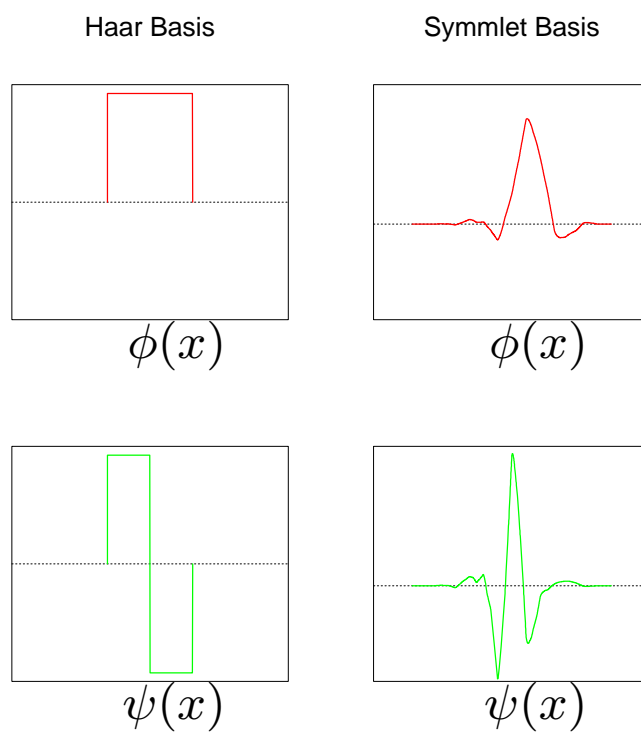


FIGURE 5.18. *The Haar and symmlet father (scaling) wavelet $\phi(x)$ and mother wavelet $\psi(x)$.*

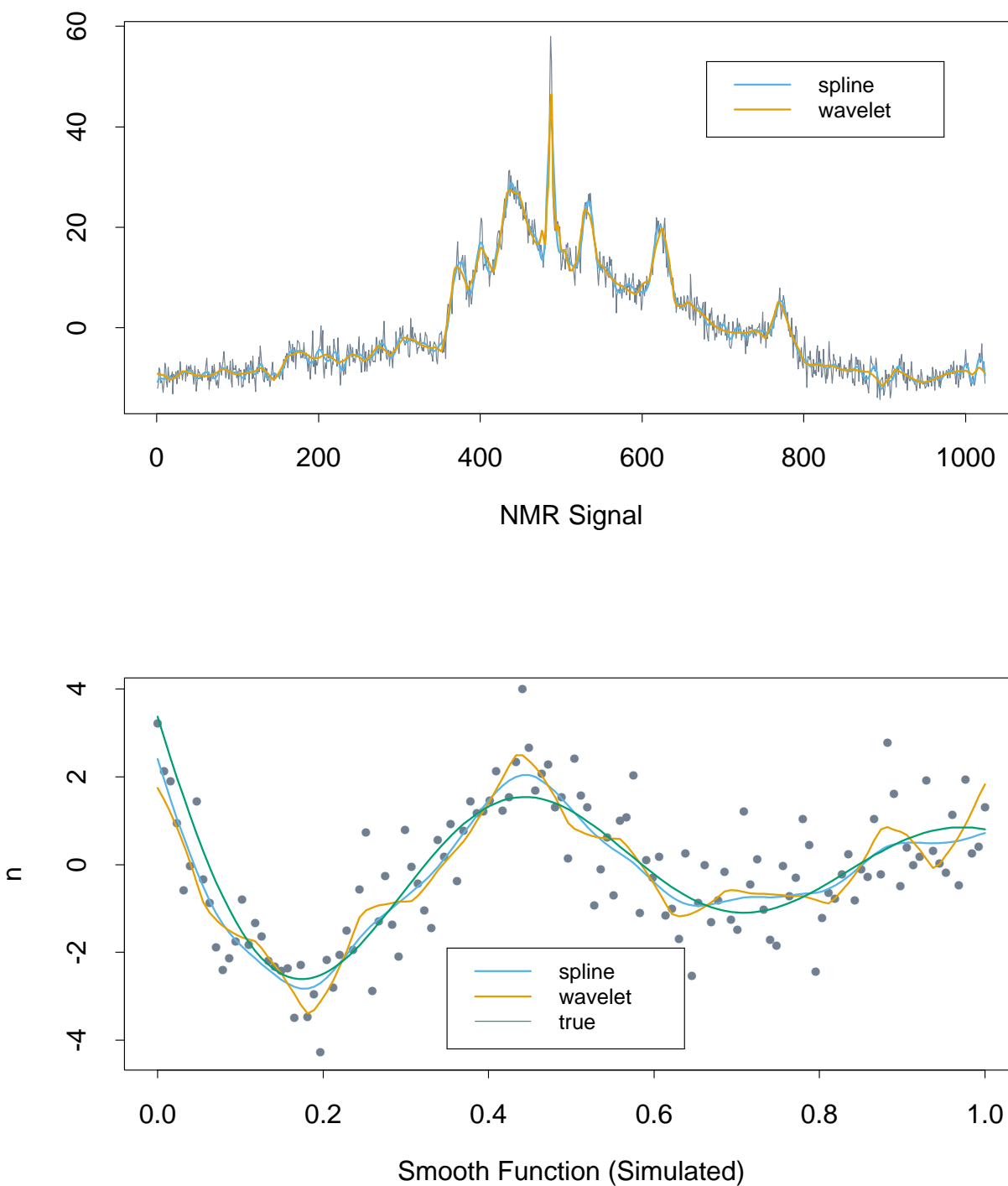


FIGURE 5.19. *Wavelet smoothing compared with smoothing splines on two examples. Each panel compares the SURE-shrunk wavelet fit to the cross-validated smoothing spline fit.*

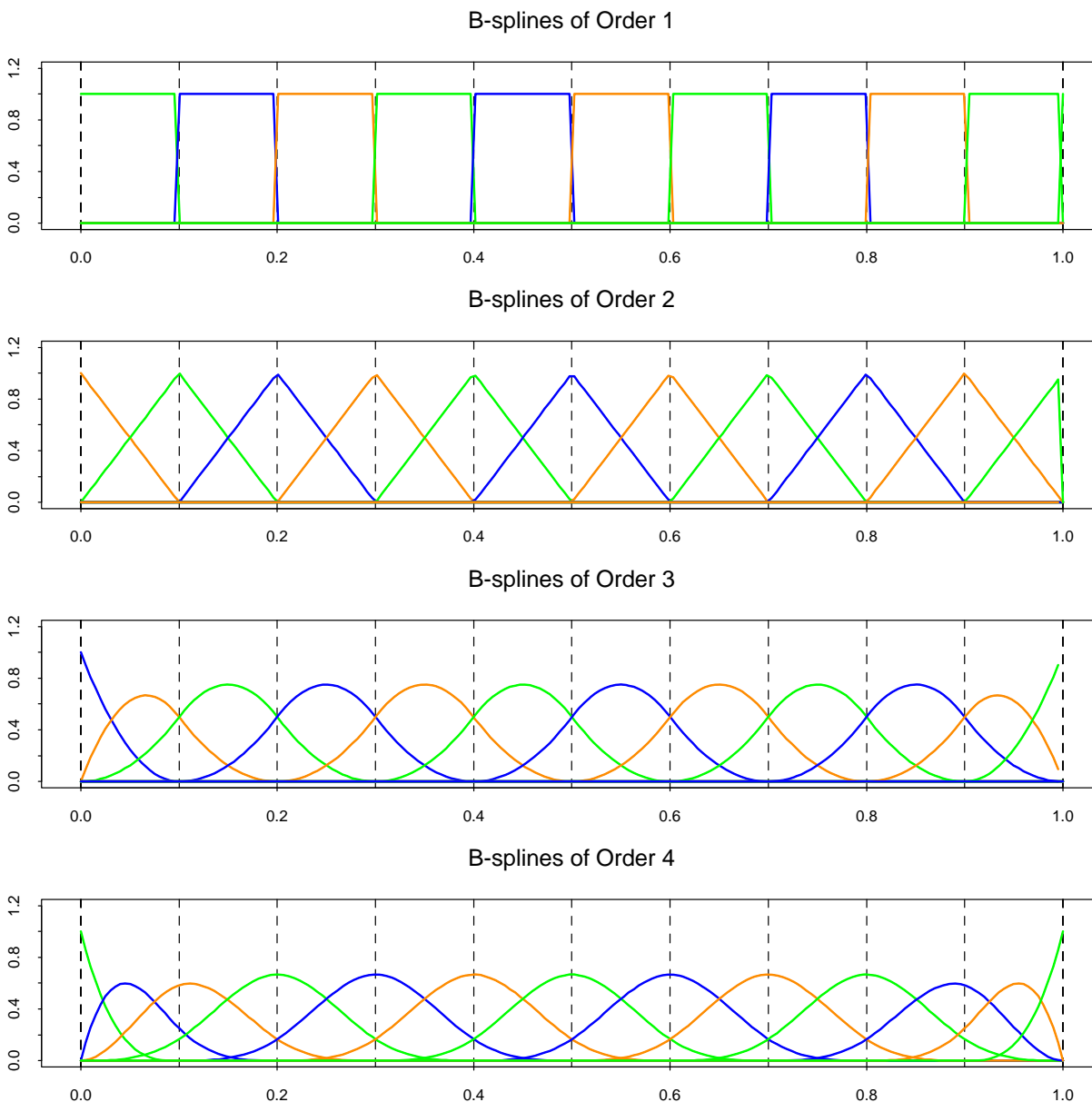


FIGURE 5.20. *The sequence of B-splines up to order four with ten knots evenly spaced from 0 to 1. The B-splines have local support; they are nonzero on an interval spanned by $M + 1$ knots.*